

Identification of the Effective Radiative Properties of Cylindrical Packed Bed Porous Media

CHAIMA BOURAOUI, FAYÇAL BEN NEJMA
Ionized and Reactive Media Studies Research Unit,
Preparatory Institute of Engineering Studies of Monastir,
Ibn Eljazzar Street, 5019
TUNISIA

Abstract: - Understanding radiative exchange in a porous medium is a crucial step that can provide significant insights and improvements in its characteristics, enhancing its practical utility across various industrial applications. In this paper, a numerical model, utilizing the finite element method (FEM), was developed to predict the radiative transfer between a diffusely/specularly reflecting cylindrical packed bed porous medium and a plane heating surface. Four different structures of the medium were suggested to examine the effect of the particles' disposition on the radiative properties of the medium. The assessment of normalized flux distribution enables the computation of effective radiative properties including reflectivity, transmissivity, and absorptivity for particles exhibiting diffuse and specular reflection. The results underscore the significant influence of particle arrangement on media properties. The structure of the second model allowed for the attainment of an opaque surface from the first layer. Meaningful correlations can be established from the presented curves, offering a streamlined and accurate method for determining effective radiative property coefficients based on emissivity in future model applications.

Key-Words: - Porous media, cylindrical packed bed, particles disposition, numerical model, FEM, radiative properties, diffuse and specular reflection.

Received: April 19, 2023. Revised: November 11, 2023. Accepted: December 19, 2023. Published: January 26, 2024.

Nomenclature:

e	Porosity
I	Radiative intensity $W.m^{-2}$
L	Characteristic length, m
\vec{n}	Normal vector
q_N	Normalized radiant flux density
q_r	Radiant flux density, $W.m^{-2}$
R	Radius of the particle
S_1	Radiant hot surface (m^2)
S_2	Radiant cold surface (m^2)
T_p	Temperature of the particles, K
T_{rad}	Temperature of the surface S_1 , K
T_s	Temperature of the surface S_2 , K

Greek Symbols:

α	Local effective absorptivity
α_{eq}	Mean effective absorptivity
ρ	Local effective reflectivity
ρ_{eff}	Mean effective reflectivity
τ	Local effective transmissivity
τ_{eff}	Mean effective transmissivity
ε	Emissivity
ε_{eff}	Mean effective emissivity
Ω	Solid angle, sr

Subscripts

b	Black body
-----	------------

1 Introduction

Radiative heat transfer in porous media is an important research topic as it is widely observed and dominant in several high-temperature applications such as catalytic combustion [1], heat exchangers [2], solar thermochemical reactors [3], medical applications [4]. The determination and understanding of the radiative properties of the

porous medium are thus key steps for the efficient design and operation of these applications.

A porous media is characterized by a complex structure of pores with irregular sizes, shapes, and connections. Therefore, the determination of its radiative characteristics has remained a complicated task. The most common assumption proposed in the literature is to consider the porous medium as a packed bed of cylinders, squares, spheres, and even a mixture of them, etc ... This hypothesis was

adopted by a considerable amount of investigations reviewed in, [5], [6], [7]. Cylindrical packed bed configuration was frequently used in porous media radiative transfer, as it has various advantages over packed beds of other particle forms. Thanks to its axisymmetric condition, it offers simplified mathematical modeling, ease of manufacture, good packing efficiency and enhanced mass transfer, etc... To solve the problem of radiative transfer in such a complex structure, porous media have been treated as a continuous and homogenous system and the standard Radiative Transfer Equation RTE has been used with “effective radiative properties”, [8], [9].

Previous research showed that reliable identifications of the radiative properties of porous media have been obtained through experimental measurements as reported in, [10], [11], [12]. Although its performance, this method can be an expensive, onerous, and time-consuming task. As an alternative method, a great number of studies have proposed theoretical and analytical approaches. A considerable body of literature examining their methodologies and highlighting their assumptions, findings and limits has been reported in, [13], [14]. Recently, along with the increase in computational capacity and speed, some authors have suggested numerical simulations for the determination of radiative properties of porous media including Monte Carlo methods, [15], [16], the Mie theory [17], Finite Volume Method (FVM) [18], discrete ordinate method (DOM) [19], Finite Element Method (FEM) [20], discrete dipole approximation [21]. More details about these methods can be found in the literature [22], [23], [24].

The determination of radiative properties of cylindrical packed bed porous media has been the subject of long-term investigation. [25], investigated the radiative heat transfer in participating media composed of long cylindrical fibers with a diameter within the geometrical optics limit. The suitability of the Single and Multi-RTE Approaches was examined by comparing the macroscopic optical properties they yielded specifically, the radiative flux, transmittance, and reflectance, with those obtained through direct Monte Carlo simulation on analogous morphologies. The results indicated that the multi-RTE approach is better suited for fibrous media with high porosity, whereas the single-RTE approach is more appropriate for isotropic fibrous media. [26], evaluated the radiative characteristics of a set of cylindrical fibers with an arrangement comparable to that of bird feathers using the Monte Carlo method. The influence of different parameters including the diameter, the volume fraction, the color, and the arrangement of the fiber as well as the

rachis's angle relative to the skin, the angle between the barb and the rachis, and the angle between the barbon and the barbules on the radiative properties of the fiber was examined. [27], suggested the addition of spherical or cylindrical particles that interact with IR radiation in the polymer matrix to improve its thermal insulation performance. In their study, a model was created to study the impact of adding the particles on the conductive and radiative properties of the opacified foam and to identify the key parameters for effective particles. Experimental tests on powders incorporated into polystyrene thin films confirmed the efficiency of the proposed solution. [28] and [29], concluded that utilizing hollow cylindrical double-layer porous media with suitable pore size and number led to improvements in the combustion temperature and the efficiency of hydrogen production.

For the past few years, there has been considerable interest in numerical simulations using commercial software as it can efficiently handle complex geometries and material properties, supporting cost-effective and time-efficient simulations. This method enables accurate characterization, optimization, and understanding of industrial processes involving radiative heat transfer in porous media, [30], [31]. The current paper suggests employing COMSOL Multiphysics, a commercial Finite Element Method (FEM) software, to examine the radiative characteristics of four regular configurations of cylindrical packed bed porous media. The objective of this study is to establish correlations between these properties and emissivity, while also assessing the impact of particle arrangement.

2 Mathematical Modelling

2.1 Problem Configuration




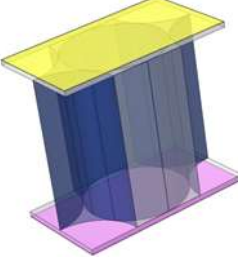
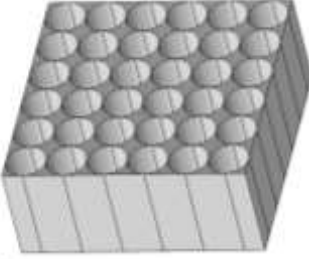

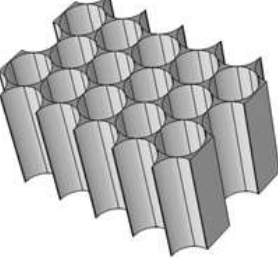
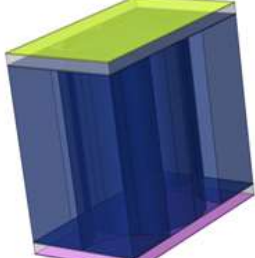
In this work, four models were considered, each consisting of a packed bed of equally sized cylinders with axes orthogonal to the radiating surface. These models differ in their particles' arrangement and thus in their porosity, as resumed in Table 1 and Table 2.

The symmetry character of these configurations allows restricting the study to their cells whose dimensions are related to the cylinder's radius by the relations listed in Table 1.

Table 1. The porosity of the configurations and the dimensions of the studied cells

Model N°	Porosity	Dimensions of the studied cells
1	$e = 1 - \frac{\pi}{4}$	$L_x = 2R$ $L_y = 2R$
2	$e = 1 - \frac{\pi}{2\sqrt{3}}$	$L_x = 2\sqrt{3}R$ $L_y = 2R$
3	$e = \frac{\pi}{4}$	$L_x = 2R$ $L_y = 2R$
4	$e = \frac{\pi}{2\sqrt{3}}$	$L_x = 2\sqrt{3}R$ $L_y = 2R$

Table 2. The details of the four studied configurations

Model N°	Arrangements of the particles	Representation of the studied cell
1		
2		
3		
4		

2.2 Hypotheses

To simplify our numerical calculations, the following hypotheses are made:

- The porous medium as well as the heating surface are infinite.
- The radiant hot surface (S_1) is considered as a black surface with the temperature T_{rad} .
- The output surface (S_2), representing the surrounding environment, is also modeled as a

black surface at a temperature $T = 0K$, neglecting its emission.

- The emissivity of the particles is negligible.

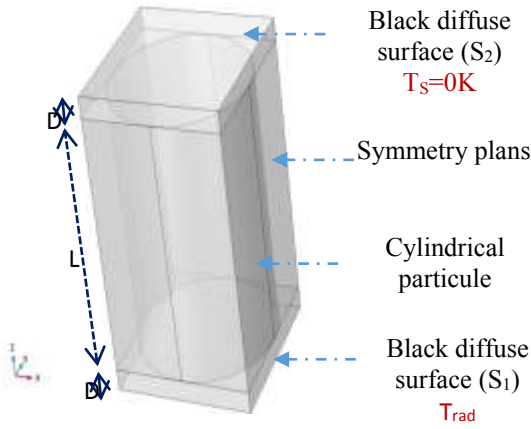


Fig. 1: The adopted assumption

When the radiation flux incident from the surface (S_1), considered as the hot surface, strikes up the porous medium surface, it undergoes three primary interactions. First, a portion of the incident radiation is reflected off the surface (S_1). Second, another fraction is absorbed by the porous medium, signifying the conversion of radiant energy into internal energy within the material. Lastly, the remaining portion, if any, is transmitted through the porous medium, reaching a second surface (S_2), as indicated in Figure 1 and Figure 2.

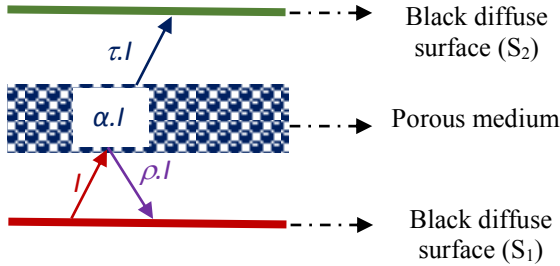


Fig. 2: The schematic presentation of the different radiative transfer by the porous media

2.3 Boundary Conditions and Equations

The present study was conducted for both types of reflection, namely diffuse and specular. The diffuse boundary condition is written as:

$$I(\vec{\Omega}) = \varepsilon I^b(T) + \frac{1-\varepsilon}{\pi} \int_{\vec{\Omega}' \cdot \vec{n} < 0} I(\vec{\Omega}') \xi(\vec{\Omega}') d\Omega' \quad (1)$$

Concerning the specular boundary condition, it can be defined as:

$$I(\vec{\Omega}) = \varepsilon I^b(T) + (1-\varepsilon)I(\vec{\Omega}') \quad (2)$$

These equations present the outgoing radiance which is composed of the emitted radiance by the surface itself (the first term) and the reflected radiance (the second term) in the case of a diffuse reflection (Eq (1)) and of a specular reflection (Eq (2)).

Where I^b is the radiative intensity of a black body, which is given by:

$$I^b = \frac{\sigma T^4}{\pi} \quad (3)$$

The radiative flux density is generally expressed as:

$$q_r = \int_{4\pi} I(\vec{\Omega}) \xi(\vec{\Omega}) d\Omega \quad (4)$$

Given the different dispositions of the particles in the studied models, a normalization of the flux has been performed. It can be calculated by:

$$q_N = \frac{q_r}{\sigma T_{rad}^4} \quad (5)$$

The local effective reflectivity is expressed as:

$$\rho = 1 - \frac{q_r(S_1)}{\sigma T_{rad}^4} \quad (6)$$

Therefore, the mean effective reflectivity can be determined by:

$$\rho_{eff} = 1 - \frac{\int_0^{L_x} \int_0^{L_y} q_r(S_1) dy dx}{L_x L_y \sigma T_{rad}^4} \quad (7)$$

For the local effective transmissivity, it is expressed as:

$$\tau = \frac{q_r(S_2)}{\sigma T_{rad}^4} \quad (8)$$

The mean effective transmissivity is thus calculated by:

$$\tau_{eff} = \frac{\int_0^{L_x} \int_0^{L_y} q_r(S_2) dy dx}{L_x L_y \sigma T_{rad}^4} \quad (9)$$

Considering the following relation:

$$\rho_{eff} + \tau_{eff} + \alpha_{eff} = 1 \quad (10)$$

The effective absorptivity can be determined using the relation:

$$\alpha_{eff} = 1 - \rho_{eff} - \tau_{eff} \quad (11)$$

2.4 Numerical Procedure

Three-dimensional geometries were generated and simulated utilizing the software COMSOL Multiphysics, employing the finite element method.

An adaptive triangular mesh was used with a refinement near the contact points between the black diffuse surface and the cylinder to get a better resolution in this area.

To ensure the independence of the solution on the grid size, different grid densities were tested by varying the boundary and edge elements. After comparing the stability of the obtained results, a grid size of 28610 boundary elements and 1812 edge elements was fixed, as it represents a good compromise between the accuracy and the time calculation. Figure 3 shows the grid structure adopted for Model 1.

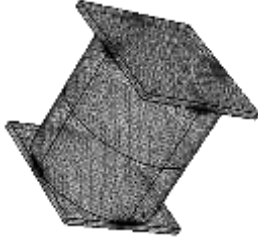


Fig. 3: The mesh grid adopted for Model 1 ($L=2R$, $D=R/10$)

3 Results and Discussions

This section entails an examination of the radiative transfer within cylindrical packed bed porous media, and more precisely the reflection, transmission, and absorption phenomena. Both diffuse and specular reflections are considered in

this analysis. Furthermore, the impact of the emissivity of the cylinders and the number of layers present is also explored.

The initial step in establishing our radiative properties involves the computation and presentation of the radiative flux. Due to the different disposition of the particles in the proposed models, a normalization of the flux has been performed to ensure consistency. Figure 4, Figure 5, Figure 6 and Figure 7 depict the normalized flux distribution at the inlet, outlet, and on the cylinders within the four models. The assessments were carried out while taking into account cylindrical particles that exhibit both diffuse and specular reflections, and possess an emissivity value of $\epsilon=0.5$. It can be seen that, at the inlet and the outlet of the four models and as the rays enter and exit the cylinder, a circular flux profile that gradually expands moving away from the cylinder's perimeter is generated. Nevertheless, the intensity of the flux distribution differs among the different proposed models. Indeed, for models 1 and 2, the flux intensity rises gradually as one moves away from the perimeter of the cylinder's face regarding the radiation emitted from neighboring particles through reflected rays.

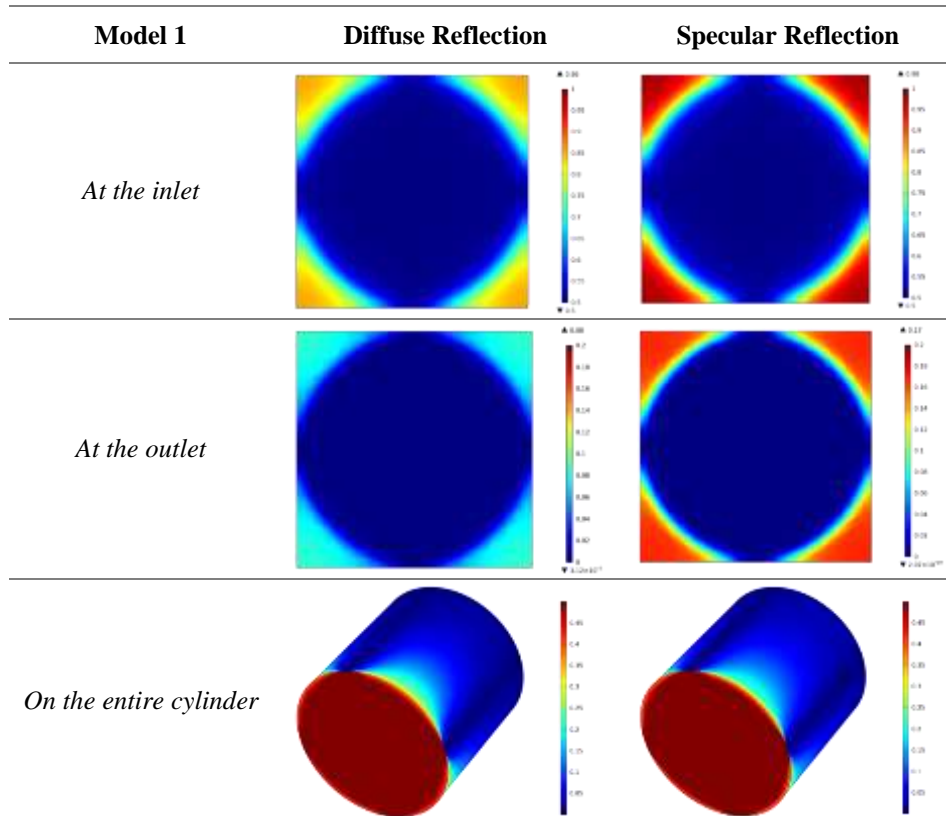


Fig. 4: the normalized flux distribution at the inlet, outlet and on the cylinders obtained for: Model 1 with $L=2R$, $D=R/10$, $\epsilon=0.5$ and for diffuse and specular reflections

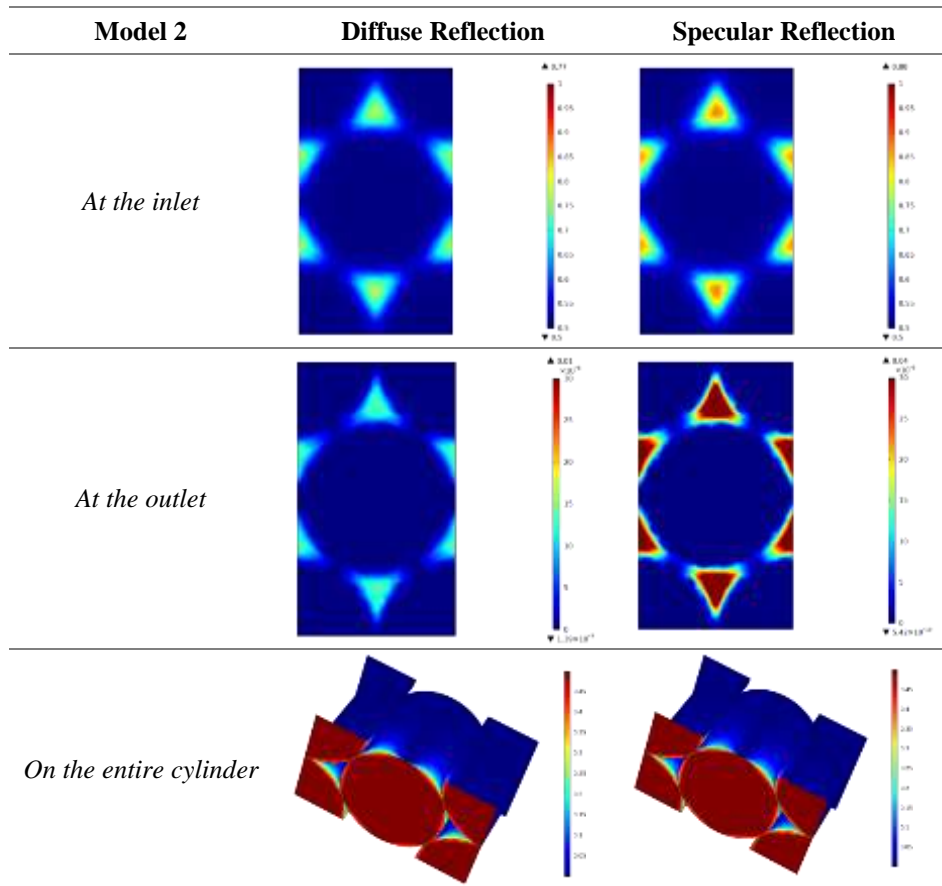


Fig. 5: the normalized flux distribution at the inlet, outlet and on the cylinders obtained for: Model 2 with $L=2R$, $D=R/10$, $\varepsilon=0.5$ and for diffuse and specular reflections

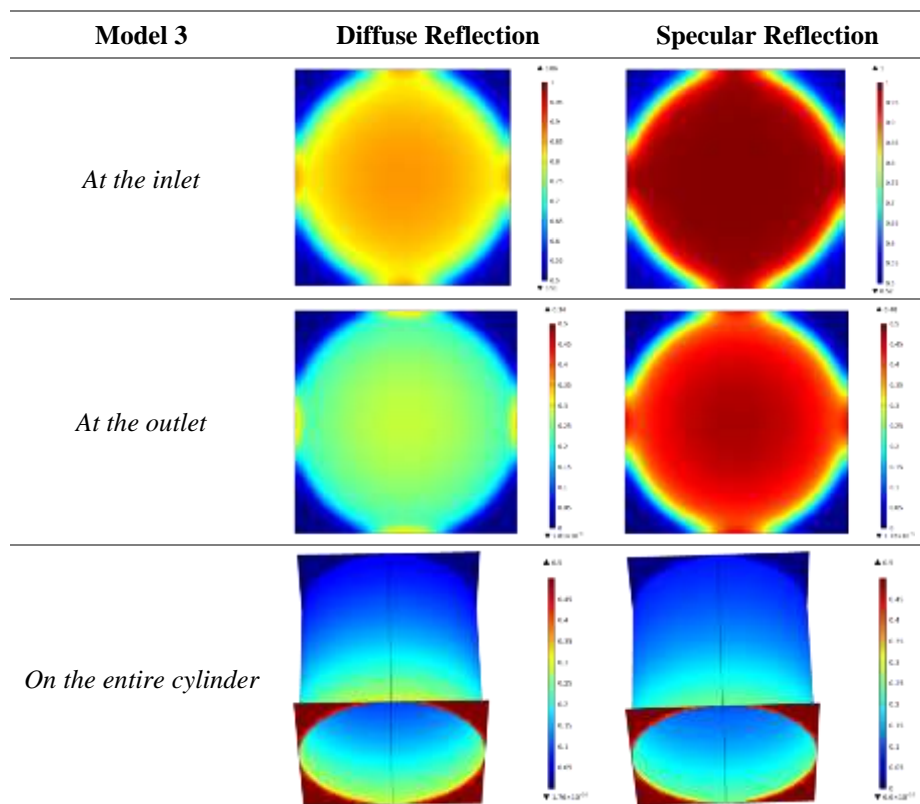


Fig. 6: the normalized flux distribution at the inlet, outlet and on the cylinders obtained for: Model 3 with $L=2R$, $D=R/10$, $\varepsilon=0.5$ and for diffuse and specular reflections

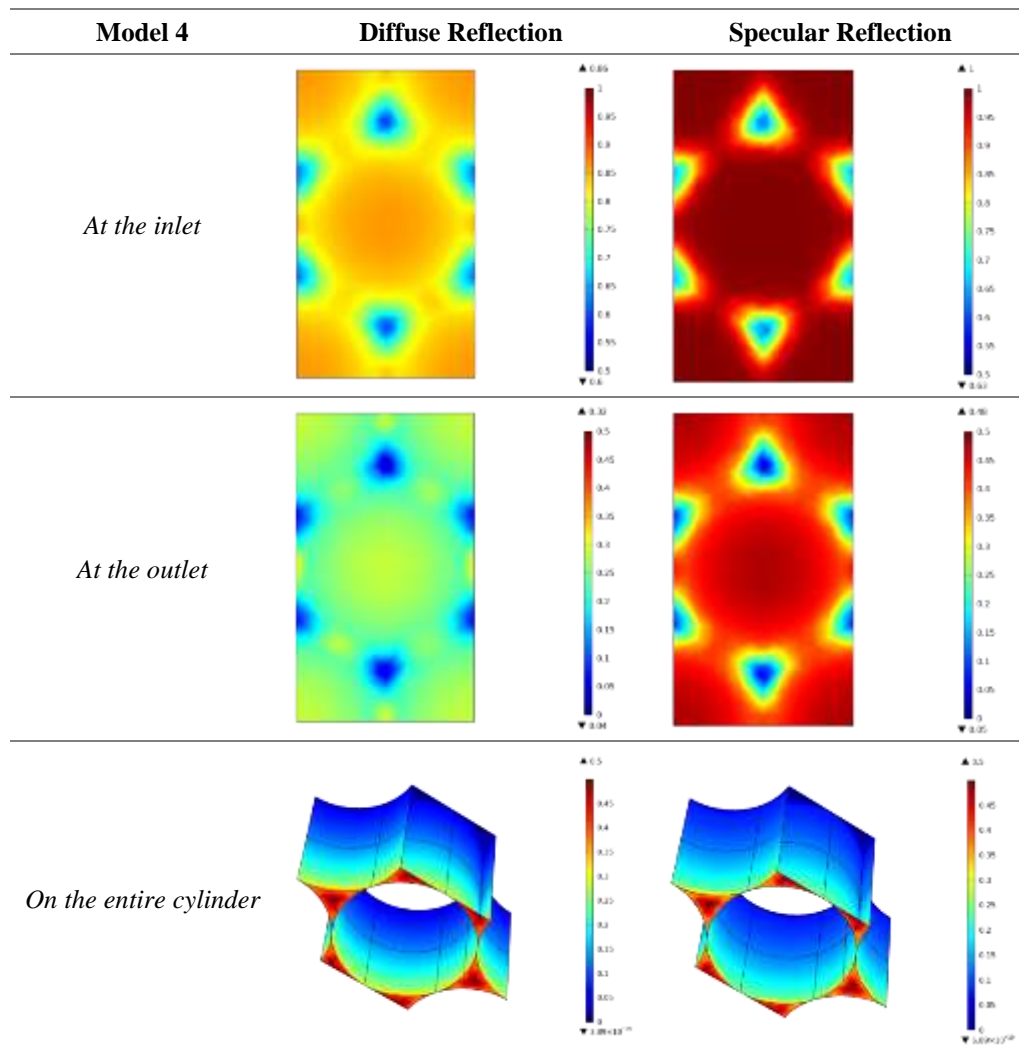


Fig. 7: the normalized flux distribution at the inlet, outlet and on the cylinders obtained for: Model 4 with $L=2R$, $D=R/10$, $\varepsilon=0.5$ and for diffuse and specular reflections

However, it exhibits an inverse trend for models 3 and 4. The flux exhibits a lower intensity at the regions where the particles are connected. Conversely, the holes formed by the arrangement of particles display a significantly higher flux intensity due to the radiation emitted by adjacent particles in all directions. These findings clearly show that the cylinders 'disposition has an impact on the flux distribution.

The distribution of flux is comparable for both particles exhibiting diffuse and specular reflection, although there is a diminished intensity in the case of diffuse reflection. This is because when light rays hit diffusely reflecting particles, they scatter in multiple directions instead of a single angle as with specularly reflecting particles. As a result, fewer rays are transmitted through diffusely reflecting particles, leading to a decrease in the flux intensity.

The distribution of the flux over the entire cylinder illustrates that the outer surface of the particles in all four models receives a greater flux

compared to the inner surface. This can be attributed to the radiation emitted by neighboring particles in the second layer.

These findings hold importance in comprehending the dynamics of radiative transfer within the suggested configurations. This knowledge bears relevance in various fields such as radiative heat transfer, transport phenomena, materials science, and engineering, as the ability to regulate energy distribution is crucial for enhancing system performance.

Based on these results, the effective reflectivity, which encapsulates both diffuse and specular reflections, was calculated and graphically depicted in Figure 8, Figure 9, Figure 10 and Figure 11 against the corresponding emissivity values. The trends observed in these figures reveal a notable inverse relationship: as the emissivity of the porous media increases, there is a discernible decrease in the amount of incident radiation being reflected. This behavior is consistent with the fundamental

principles of emissivity and reflectivity, where higher emissivity values signify an increased capacity for a material to absorb and emit radiation, consequently leading to reduced reflectivity. Moreover, it is noteworthy that the observed relationship between emissivity and reflectivity aligns with fundamental principles governing radiative heat transfer. Surfaces with emissivity values approaching zero, as noted in the instances of highest reflectivity, signify a diminished capacity to absorb and emit radiation. This phenomenon can be attributed to the fact that materials with low emissivity tend to reflect a larger proportion of incident radiation, resulting in heightened reflectivity. Conversely, a surface characterized by an emissivity value of 1, characteristic of a black body, exhibited a complete absence of reflectivity. This behavior adheres to the theoretical expectation for a black body, which absorbs all incident radiation without reflecting any.

Furthermore, the influence of the internal disposition of the cylindrical particles within the porous media was underscored. It was shown that, in the case of diffusely reflected particles, the first six layers of models 1, 3, and 4 contributed to the reflection of the incident radiation. Indeed, the arrangement of the particles in each layer creates additional interfaces for scattering and reflection, contributing to an increased likelihood of diffusely reflected particles encountering surfaces conducive to reflection. This phenomenon results in a higher overall reflectivity compared to the scenario with a single layer, where the opportunities for multiple interactions and reflections are limited. In contrast, for the specularly reflected particles in the four models and diffusely reflected particles in model 2, the first layer of the porous medium surface emerges as the main reflecting surface. This can be attributed to its smoothness and the medium structure.

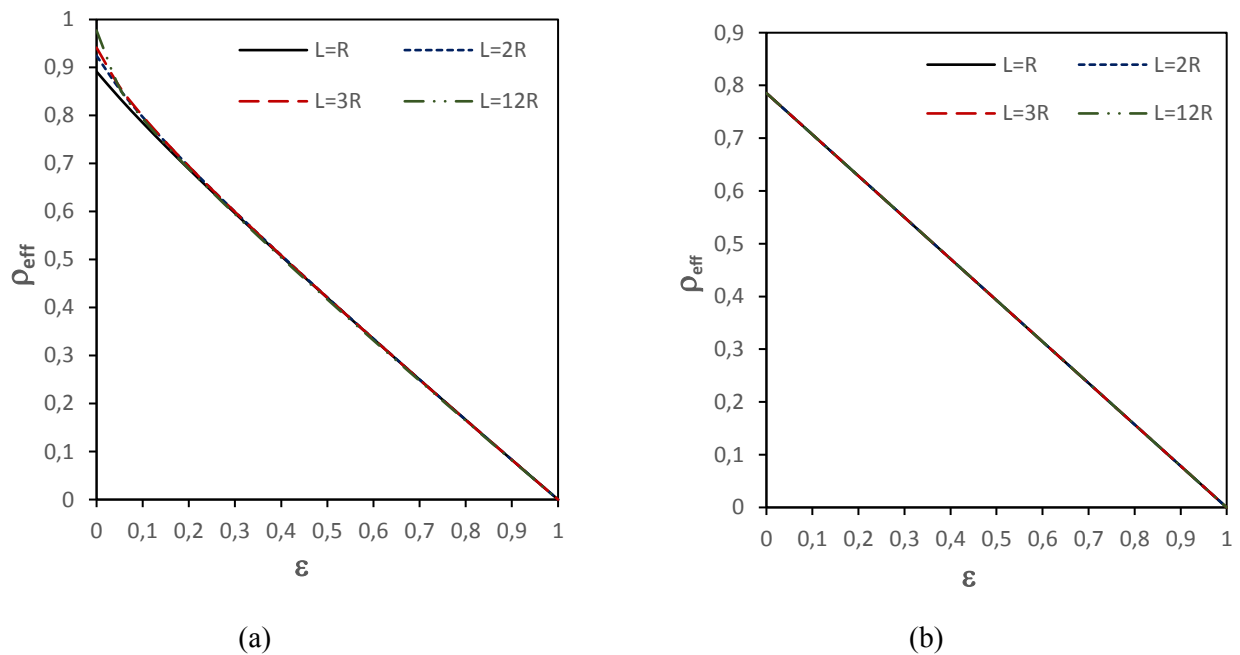


Fig. 8: Variation of effective reflectivity with emissivity for diffuse (a) and specular (b) reflecting cylindrical particles in Model 1 across different Layers

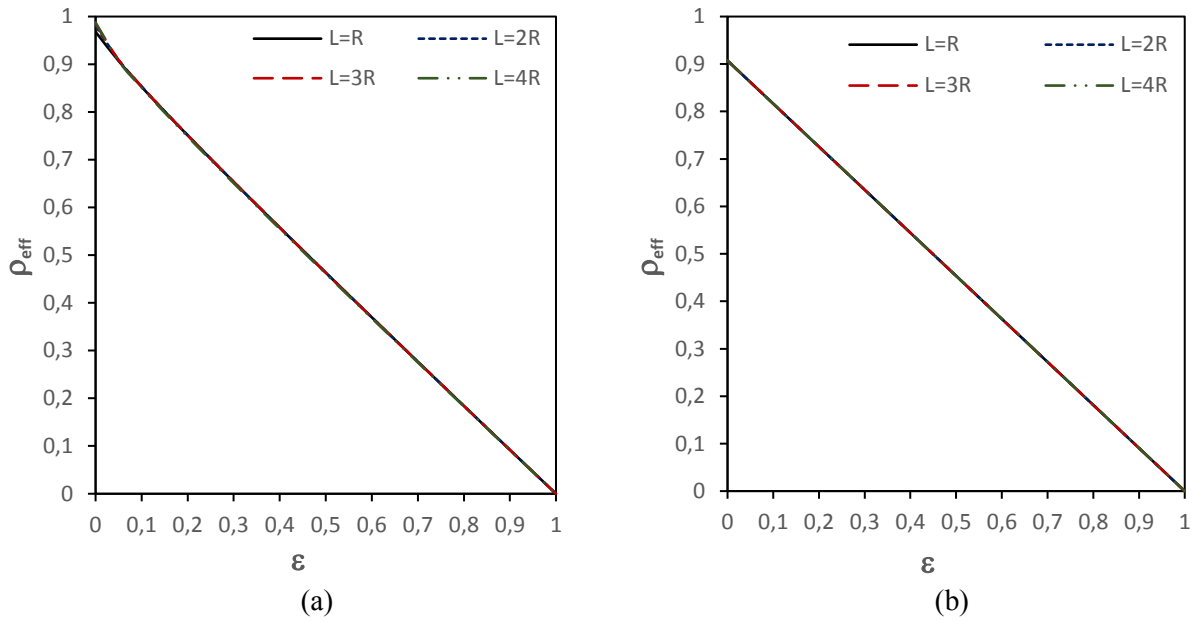


Fig. 9: Variation of effective reflectivity with emissivity for diffuse (a) and specular (b) reflecting cylindrical particles in Model 2 across different Layers

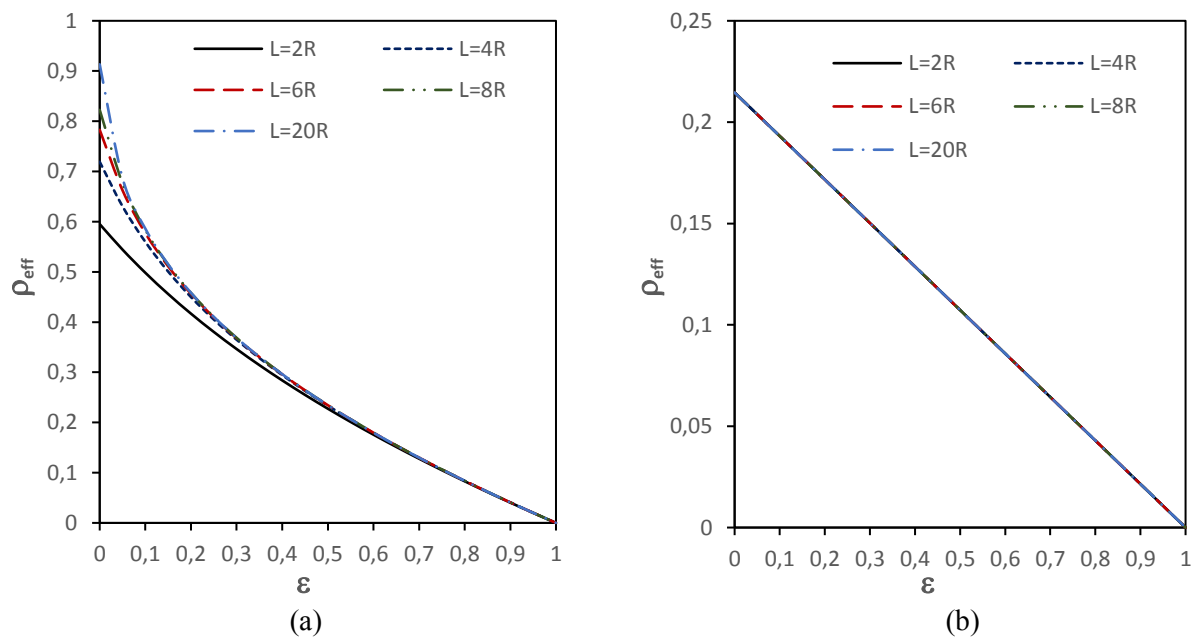


Fig. 10: Variation of effective reflectivity with emissivity for diffuse (a) and specular (b) reflecting cylindrical particles in Model 3 across different Layers

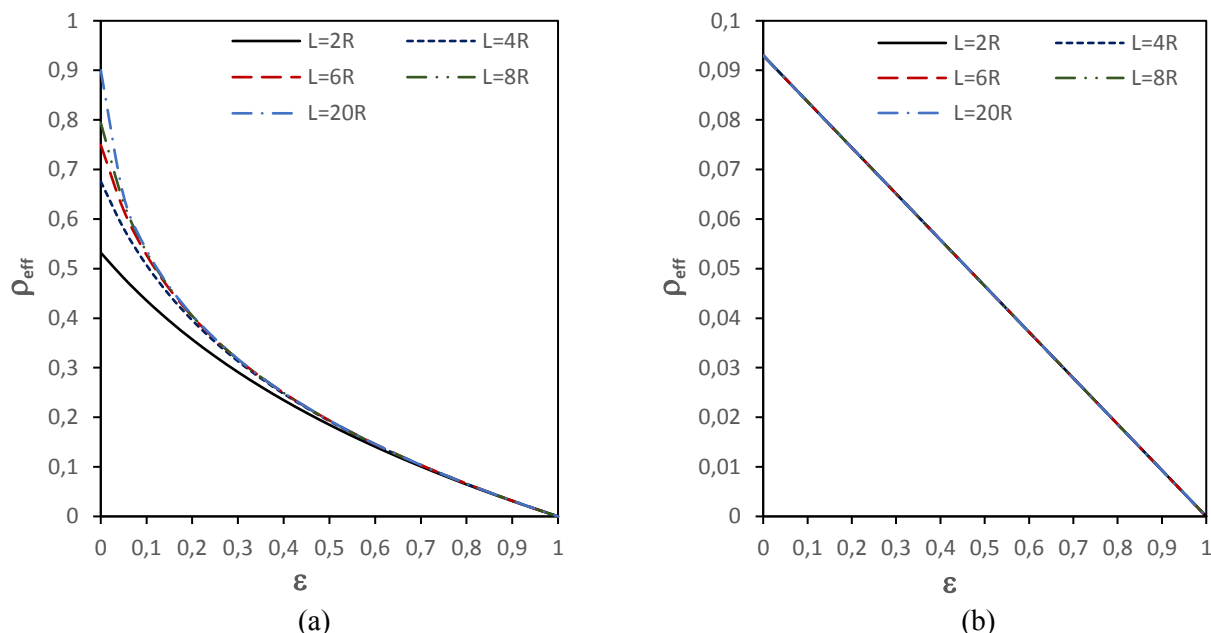


Fig. 11: Variation of effective reflectivity with emissivity for diffuse (a) and specular (b) reflecting cylindrical particles in Model 4 across different Layers

Using the obtained curves of the effective reflectivity for the four models, correlations linking the effective reflectivity coefficient and the emissivity have been established for specular reflection, as illustrated in Table 3. This insight is crucial, particularly for engineers and scientists working on energy-efficient building design. Such relationships enable informed material selection, optimizing the balance between reflectivity and emissivity for enhanced control over heat transfer. This has practical applications in diverse areas, including thermal insulation, solar panels, building materials, etc...

Table 3. The correlations of effective reflectivity in the case of specular reflection

Model N°	Effective reflectivity
1	$\rho_{eff} = (1 - \epsilon) * \frac{\pi}{4}$
2	$\rho_{eff} = (1 - \epsilon) * \frac{\pi}{2\sqrt{3}}$
3	$\rho_{eff} = (1 - \epsilon) * (1 - \frac{\pi}{4})$
4	$\rho_{eff} = (1 - \epsilon) * (1 - \frac{\pi}{2\sqrt{3}})$

Under the assumption that the radiating surface uniformly emits radiation to the porous medium, the calculation and plotting of transmissivity for different layers, corresponding to the four models, were performed as a function of emissivity for both reflection cases. The results, presented in Figure 12, Figure 13, Figure 14 and Figure 15, indicated a

decrease in transmissivity with an increase in emissivity, a trend particularly pronounced as the number of layers escalates, leading to a faster convergence of transmissivity curves towards zero.

In addition, a comparative analysis of the obtained transmissivity curves for the four suggested models revealed the significant impact of model structure on transmissivity. Figure 13 highlights that Model 2, with its unique structural configuration, exhibits an abrupt transition to an almost complete opacity starting from the second layer. This can be attributed to the closely packed nature of the particles in each layer, hindering the transmission of radiation through the medium. However, as presented in Figure 12, Figure 14 and Figure 15, opacity begins to manifest from the sixth layer for Model 1 and the tenth layer for Models 3 and 4. This can be ascribed to the looser packing arrangement of the particles and the existence of numerous voids among them.

It can also be noted that a specular surface tends to have higher transmissivity than a diffuse surface. This is because specular reflection involves minimal scattering, allowing more radiation to pass through the material. In contrast, a diffuse surface scatters radiation in multiple directions, which can result in a portion of the radiation being absorbed or redirected away from the original path, reducing transmissivity.

In this study, the investigated media were treated as opaque surfaces. Consequently, the utilization of effective properties is deemed justified for this purpose.

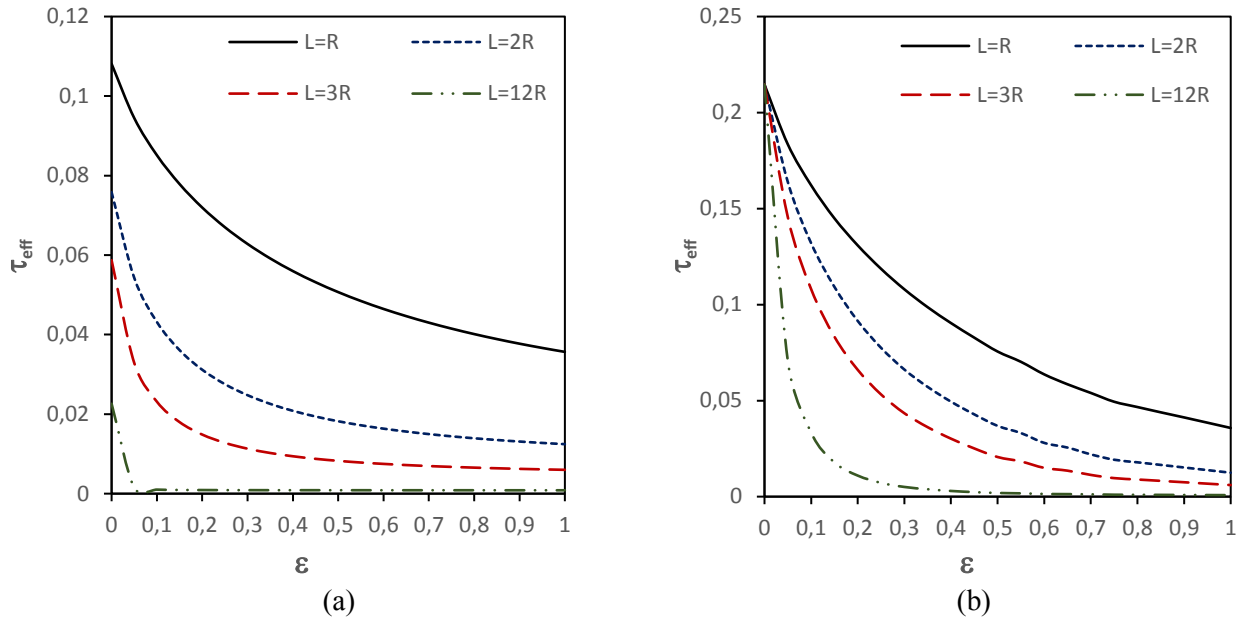


Fig. 12: Variation of effective transmissivity with emissivity for diffuse (a) and specular (b) reflecting cylindrical particles in Model 1 across different Layers

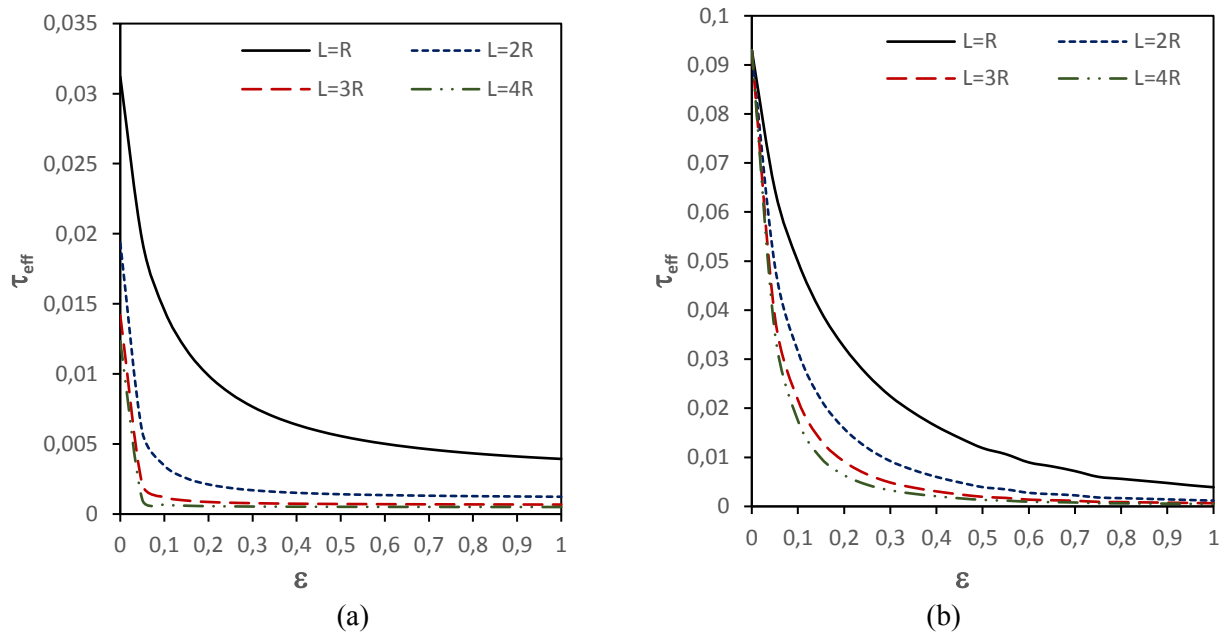


Fig. 13: Variation of effective transmissivity with emissivity for diffuse (a) and specular (b) reflecting cylindrical particles in Model 2 across different Layers

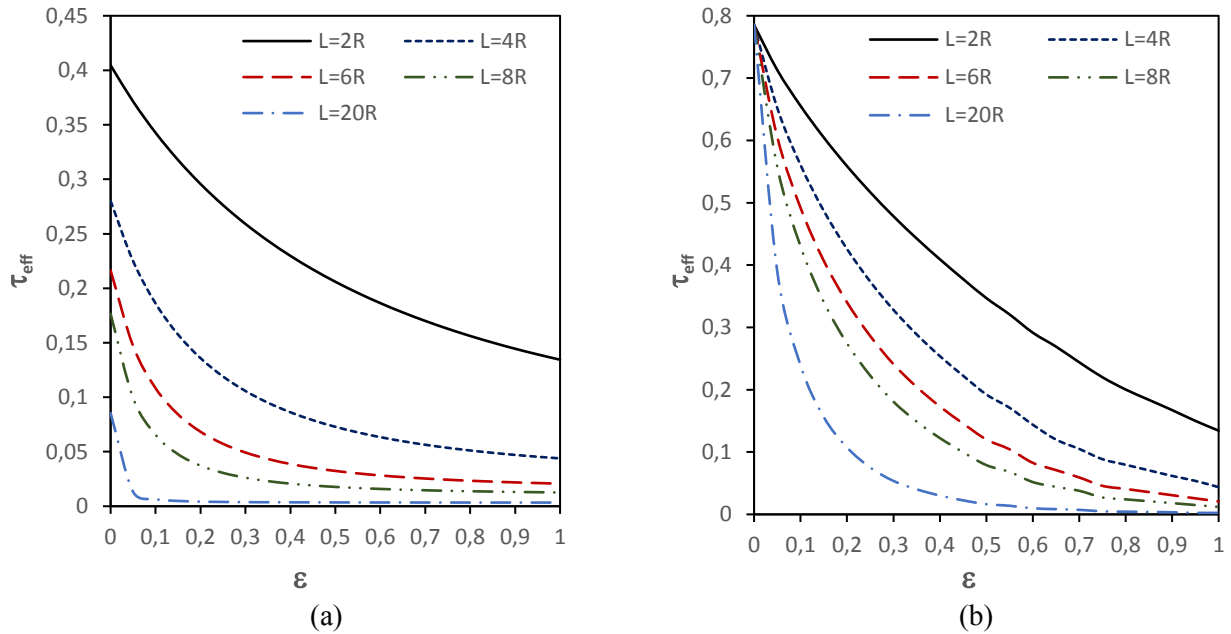


Fig. 14: Variation of effective transmissivity with emissivity for diffuse (a) and specular (b) reflecting cylindrical particles in Model 3 across different Layers

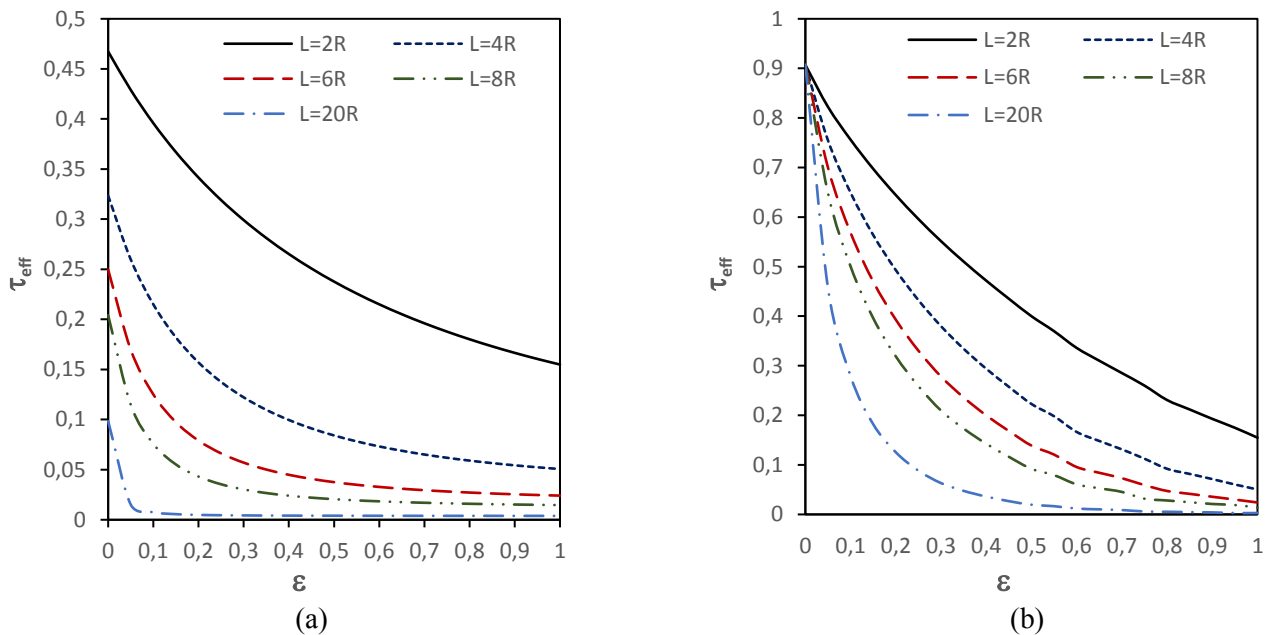


Fig. 15: Variation of effective transmissivity with emissivity for diffuse (a) and specular (b) reflecting cylindrical particles in Model 4 across different Layers

The effective absorptivity is also computed and graphically represented as a function of emissivity for the four models and considering both reflection cases, as depicted in Figure 16, Figure 17, Figure 18 and Figure 19. With an increase in emissivity, coupled with the presence of voids in each model, there is an augmentation in the likelihood of radiation being absorbed by the particles.

The particles within the bed not only absorb incident radiation but also have the potential to

receive radiation emitted by neighboring particles and reflected within the voids. This intricate interplay contributes to the overall increase in absorptivity. The heightened emissivity, in conjunction with the structural characteristics of the bed, facilitates a more effective interaction with thermal radiation, underscoring the nuanced dynamics at play in the absorption process.

Additionally, it is important to underscore that a substantial portion of radiation was absorbed by the

cylindrical particles located in the initial layers of the porous media. To be more precise, upon comparing the absorptivity curves derived for the four models under both reflection scenarios, it is noteworthy that the first layer of Model 2, where the cylindrical particles are strategically positioned, exhibited the remarkable capability to absorb all incoming radiation. Similarly, the first layer of Model 1 absorbed nearly all the radiation, with a

minor portion being absorbed by the subsequent five layers. As for Models 3 and 4, the initial ten layers played a significant role in the absorption of radiation, particularly in the case of specular reflection. This variation in absorption behavior can be attributed to the specific geometric configuration and distribution of the cylindrical particles in each model, emphasizing the nuanced impact of particle arrangement on radiation absorption.

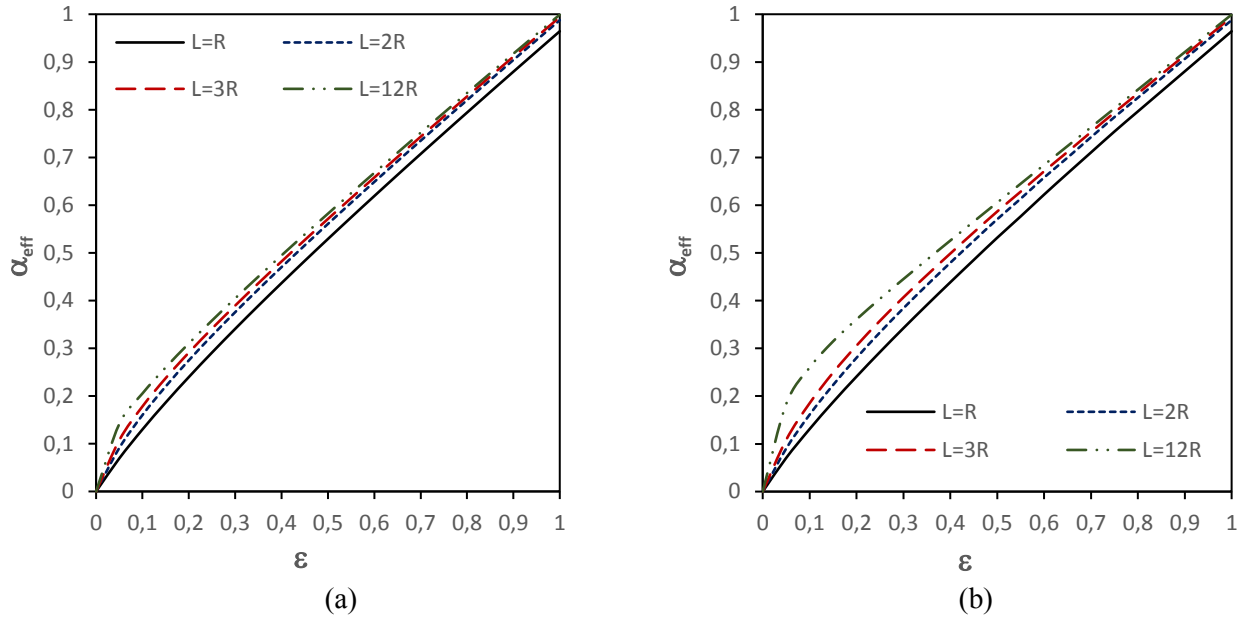


Fig. 16: Variation of effective absorptivity with emissivity for diffuse (a) and specular (b) reflecting cylindrical particles in Model 1 across different Layers

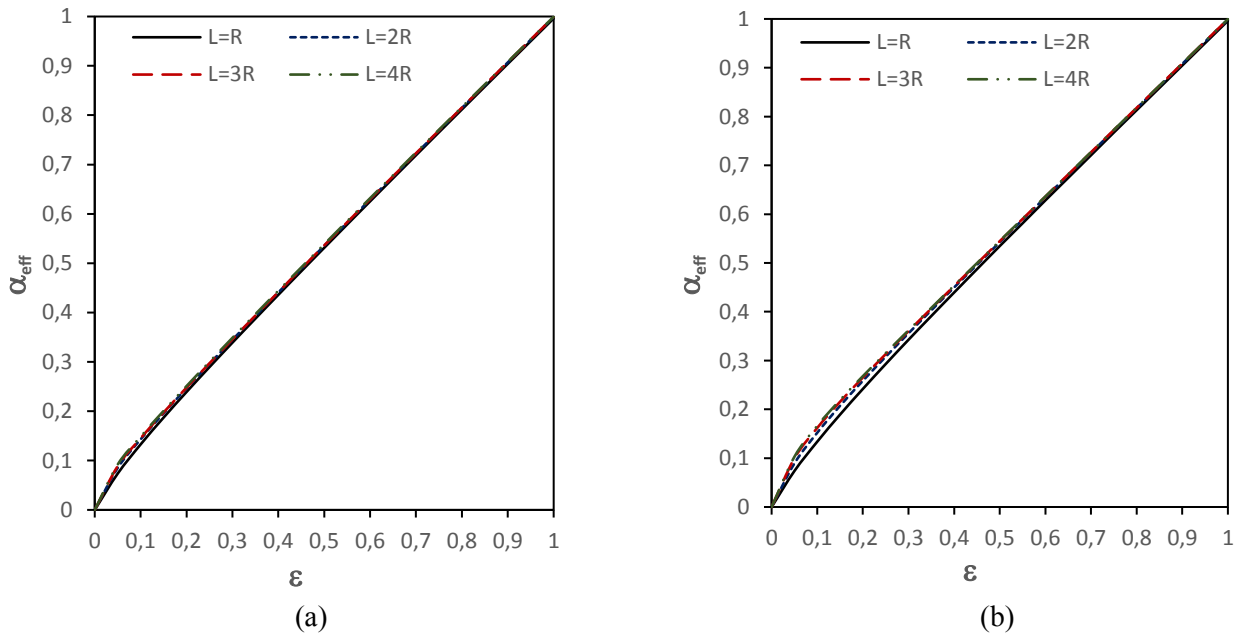


Fig. 17: Variation of effective absorptivity with emissivity for diffuse (a) and specular (b) reflecting cylindrical particles in Model 2 across different Layers

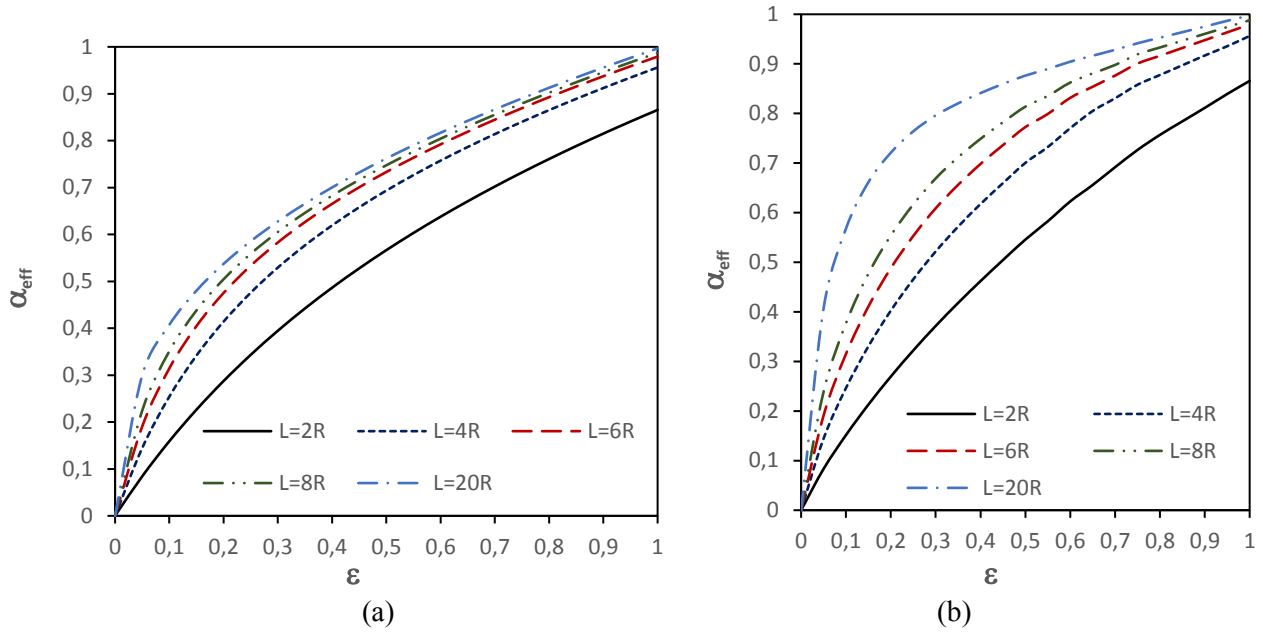


Fig. 18: Variation of effective absorptivity with emissivity for diffuse (a) and specular (b) reflecting cylindrical particles in Model 3 across different Layers

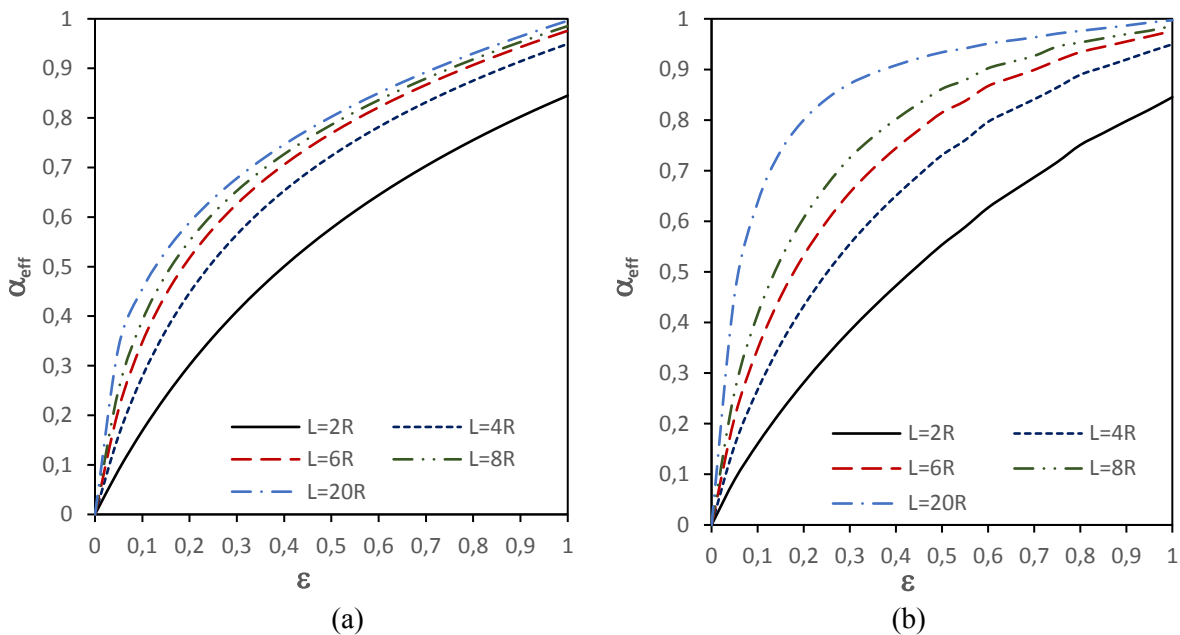


Fig. 19: Variation of effective transmissivity with emissivity for diffuse (a) and specular (b) reflecting cylindrical particles in Model 4 across different Layers

These findings provide valuable insights into the impact of internal structural variations on the radiative behavior of porous media. Such considerations are crucial in the design and optimization of materials for applications involving radiative heat transfer, offering a nuanced understanding of how internal configurations can affect the overall thermal performance of porous media. For instance, in the heating, ventilation and air conditioning (HVAC) field, this can lead to the

development of advanced heat exchange systems and HVAC components. This knowledge can be applied to design more efficient thermal insulation for buildings, improving temperature regulation and reducing energy consumption. Additionally, it can contribute to the enhancement of HVAC systems, allowing for better control of indoor temperatures and increased energy efficiency in both residential and commercial settings. The implications extend to the automotive industry, where optimized thermal

management systems can improve engine efficiency and overall vehicle performance.

By comparing the obtained results to those presented in another study on spherical packed bed porous media [32], it can be noted that spherical packed configurations facilitate the quicker attainment of an opaque medium. They also appear to be more reflective and absorptive in comparison to a cylindrical packed bed porous media.

4 Conclusion

Numerical simulations were performed to assess the radiative properties of four configurations of cylindrical packed bed porous media, considering both specular and diffusive reflection of particles. Employing a COMSOL Multiphysics model, the impact of the arrangement of particles was conducted. The normalized flux calculations revealed circular flux profiles with varying intensities across the proposed models. The first layer of Model 2 emerges as the main reflecting, transmitting and absorbing surface, whereas the other models required multiple layers to achieve complete radiation reflection, resulting in an opaque medium. These layers also contributed in the absorption of radiation.

This approach, grounded in numerical simulation calculations, provides an efficient and cost-effective alternative to analytical and experimental methods, offering insights into the complex nature of radiative heat transfer through porous media.

References

- [1] P. Qian, M. Liu, X. Li, F. Xie, Z. Huang, C. Luo and X. Zhu « Combustion characteristics and radiation performance of premixed hydrogen/air combustion in a mesoscale divergent porous media combustor », *International Journal of Hydrogen Energy*, vol. 45, n° 7, p. 5002-5013, févr. 2020, doi: 10.1016/j.ijhydene.2019.12.094.
- [2] S. Rashidi, M. H. Kashefi, K. C. Kim, and O. Samimi-Abianeh, « Potentials of porous materials for energy management in heat exchangers – A comprehensive review », *Applied Energy*, vol. 243, p. 206-232, juin 2019, doi: 10.1016/j.apenergy.2019.03.200.
- [3] H. Zhang, B. Guene Lougou, R. Pan, Y. Shuai, F. Wang, Z. Cheng and H. Tan « Analysis of thermal transport and fluid flow in high-temperature porous media solar thermochemical reactor », *Solar Energy*, vol. 173, p. 814-824, oct. 2018, doi: 10.1016/j.solener.2018.08.015.
- [4] L. Dombrovsky, J. H. Randrianalisoa, W. Lipinski, and V. Timchenko, « Simplified approaches to radiative transfer simulations in laser-induced hyperthermia of superficial tumors », *CTS*, vol. 5, n° 6, 2013, doi: 10.1615/ComputThermalScien.2013008157.
- [5] W. Fuqiang, Z. Xinping, D. Yan, Y. Hongliang, X. Shi, L. Yang and C. Ziming., « Progress in radiative transfer in porous medium: A review from macro scale to pore scale with experimental test », *Applied Thermal Engineering*, vol. 210, p. 118331, juin 2022.
- [6] S. Hajimirza and H. Sharadga, « Learning thermal radiative properties of porous media from engineered geometric features », *International Journal of Heat and Mass Transfer*, vol. 179, p. 121668, nov. 2021.
- [7] H. H. Kang, « Machine Learning Implementation in Radiative Properties Prediction for Porous Media », Thesis, 2019.
- [8] M. Luo, C. Wang, J. Zhao, and L. Liu, « Characteristics of effective thermal conductivity of porous materials considering thermal radiation: A pore-level analysis », *International Journal of Heat and Mass Transfer*, vol. 188, p. 122597, juin 2022, doi: 10.1016/j.ijheatmasstransfer.2022.122597.
- [9] B. Liu, J. Zhao, and L. Liu, « Continuum approach based on radiation distribution function for radiative heat transfer in densely packed particulate system », *Journal of Quantitative Spectroscopy and Radiative Transfer*, vol. 253, p. 107028, sept. 2020.
- [10] F. Retailleau, V. Allheily, L. Merlat, J.-F. Henry, and J. H. Randrianalisoa, « Experimental characterization of radiative transfer in semi-transparent composite materials with rough boundaries », *Journal of Quantitative Spectroscopy and Radiative Transfer*, vol. 256, p. 107300, nov. 2020, doi: 10.1016/j.jqsrt.2020.107300.
- [11] F. Retailleau, V. Allheily, L. Merlat, J.-F. Henry, and J. Randrianalisoa, « Experimental study of radiative transfer in semi-transparent composite materials at different temperatures », *J. Phys.: Conf. Ser.*, vol. 2116, n° 1, p. 012062, nov. 2021, doi: 10.1088/1742-6596/2116/1/012062.
- [12] J. F. Sacadura and D. Baillis, « Experimental characterization of thermal radiation properties of dispersed media »,

- International Journal of Thermal Sciences*, vol. 41, n° 7, p. 699-707, June 2002.
- [13] S. Cunsolo, R. Coquard, D. Baillis, and N. Bianco, « Radiative properties modeling of open cell solid foam: Review and new analytical law », *International Journal of Thermal Sciences*, vol. 104, p. 122-134, June 2016.
- [14] J. Randrianalisoa and D. Baillis, « Analytical model of radiative properties of packed beds and dispersed media », *International Journal of Heat and Mass Transfer*, vol. 70, p. 264-275, mars 2014.
- [15] Y. Maanane, M. Roger, A. Delmas, M. Galtier, and F. André, « Symbolic Monte Carlo method applied to the identification of radiative properties of a heterogeneous material », *Journal of Quantitative Spectroscopy and Radiative Transfer*, vol. 249, p. 107019, juill. 2020, doi: 10.1016/j.jqsrt.2020.107019.
- [16] A. Sit, R. Wulf, T. Fieback, and P. Talukdar, « Identification of spectral radiative properties of closed cell polymeric foams using coupled Monte Carlo-particle swarm optimization », *International Journal of Thermal Sciences*, vol. 189, p. 108263, juill. 2023, doi: 10.1016/j.ijthermalsci.2023.108263.
- [17] Y. Wang, P. Hsu, and M. H. McCay, « The Pore Size Dependence of the Radiative Scattering Coefficient in Yttria-Stabilized Zirconia Films », presented at *ASME Turbo Expo 2022: Turbomachinery Technical Conference and Exposition, American Society of Mechanical Engineers Digital Collection*, oct. 2022. doi: 10.1115/GT2022-80853.
- [18] P. Zhang, C. Sun, and X.-L. Xia, « Improved Gold-SA algorithm for simultaneous estimation of temperature-dependent thermal conductivity and spectral radiative properties of semitransparent medium », *International Journal of Heat and Mass Transfer*, vol. 191, p. 122836, August 2022, doi: 10.1016/j.ijheatmasstransfer.2022.122836.
- [19] Z.-T. Niu, H. Qi, Y.-K. Ji, S. Wen, Y.-T. Ren, and M.-J. He, « Real-time reconstruction of thermal boundary condition of porous media via temperature sequence », *International Journal of Thermal Sciences*, vol. 177, p. 107570, July 2022, doi: 10.1016/j.ijthermalsci.2022.107570.
- [20] H. Gonome, « Interference effect of localized surface plasmon resonance on radiative properties of plasmonic particle clusters in 3D assemblies », *Journal of Quantitative Spectroscopy and Radiative Transfer*, vol. 230, p. 13-23, June 2019.
- [21] Y. Tang, K. Zhu, and Y. Huang, « Radiative properties of porous fly ash particles based on the particle superposition model », *Journal of Quantitative Spectroscopy and Radiative Transfer*, vol. 277, p. 107977, Jan. 2022, doi: 10.1016/j.jqsrt.2021.107977.
- [22] O. Rozenbaum, C. Blanchard, and D. De Sousa Meneses, « Determination of high-temperature radiative properties of porous silica by combined image analysis, infrared spectroscopy and numerical simulation », *International Journal of Thermal Sciences*, vol. 137, p. 552-559, march 2019.
- [23] L. Ni, Z. Chen, P. Mukhopadhyaya, X. Zhang, Q. Wu, Q. Yu and G. Miu, « Numerical simulation on thermal performance of vacuum insulation panels with fiber /powder porous media based on CFD method », *International Journal of Thermal Sciences*, vol. 172, p. 107320, févr. 2022, doi: 10.1016/j.ijthermalsci.2021.107320.
- [24] C. Chen, D. Ranjan, P. G. Loutzenhiser, and Z. M. Zhang, « A numerical study of the spectral radiative properties of packed bed with mixed bauxite and silica spheres », *International Journal of Heat and Mass Transfer*, vol. 207, p. 124025, june 2023, doi: 10.1016/j.ijheatmasstransfer.2023.124025.
- [25] J. Randrianalisoa, S. Haussener, D. Baillis, and W. Lipiński, « Radiative characterization of random fibrous media with long cylindrical fibers: Comparison of single- and multi-RTE approaches », *Journal of Quantitative Spectroscopy and Radiative Transfer*, vol. 202, p. 220-232, nov. 2017, doi: 10.1016/j.jqsrt.2017.08.002.
- [26] M. Sedghi, A. Saboonchi, and M. Ghane, « Numerical study of radiative properties of birds' feathers using Monte Carlo method », *International Communications in Heat and Mass Transfer*, vol. 117, p. 104718, oct. 2020, doi: 10.1016/j.icheatmasstransfer.2020.104718.
- [27] R. Coquard, D. Baillis, and D. Quenard, « Numerical and experimental study of the IR opacification of polystyrene foams for thermal insulation enhancement », *Energy and Buildings*, vol. 183, p. 54-63, janv. 2019, doi: 10.1016/j.enbuild.2018.10.037.

- [28] A. Maznoy, A. Kirdyashkin, S. Minaev, A. Markov, N. Pichugin, and E. Yakovlev, « A study on the effects of porous structure on the environmental and radiative characteristics of cylindrical Ni-Al burners », *Energy*, vol. 160, p. 399-409, oct. 2018, doi: 10.1016/j.energy.2018.07.017.
- [29] H. Zhu, H. Dai, Z. Song, X. Wang, Z. Wang, H. Dai, S. He, « Improvement of hollow cylinders on the conversion of coal mine methane to hydrogen in packed bed burner », *International Journal of Hydrogen Energy*, vol. 46, n° 61, p. 31439-31451, sept. 2021, doi: 10.1016/j.ijhydene.2021.07.036.
- [30] E. Codau, T.-C. Codau, I.-G. Lupu, A. Raru, and D. Farima, « Heat transfer simulation through textile porous media », *The Journal of The Textile Institute*, vol. 114, n° 2, p. 257-264, feb. 2023, doi: 10.1080/00405000.2022.2027608.
- [31] M. Sans, O. Farges, V. Schick, and G. Parent, « Solving transient coupled conductive and radiative transfers in porous media with a Monte Carlo Method: Characterization of thermal conductivity of foams using a numerical Flash Method », *International Journal of Thermal Sciences*, vol. 179, p. 107656, sept. 2022, doi: 10.1016/j.ijthermalsci.2022.107656.
- [32] C. Bouraoui and F. Ben Nejma, « Numerical simulation for the determination of the radiative properties of spherical packed bed porous media: A COMSOL Multiphysics Study », *Advances in Mechanical Engineering*, vol. 15, n° 10, p. 16878132231205724, oct. 2023, doi: 10.1177/16878132231205724.

Contribution of Individual Authors to the Creation of a Scientific Article (Ghostwriting Policy)

The authors equally contributed to the present research, at all stages from the formulation of the problem to the final findings and solution.

Sources of Funding for Research Presented in a Scientific Article or Scientific Article Itself

No funding was received for conducting this study.

Conflict of Interest

The authors have no conflicts of interest to declare.

Creative Commons Attribution License 4.0 (Attribution 4.0 International, CC BY 4.0)

This article is published under the terms of the Creative Commons Attribution License 4.0

https://creativecommons.org/licenses/by/4.0/deed.en_US